Research Article

Guanghui Zheng, Jingqing Liang, Xuehui Zheng, Xiaolong Sun*, and Hualong Xu

Impact and mechanism of improving the UV aging resistance performance of modified asphalt binder

https://doi.org/10.1515/rams-2025-0111
received August 02, 2024; accepted April 17, 2025

Abstract: To control the ultraviolet (UV) aging behavior of asphalt pavement materials effectively, hindered amine light stabilizer (HALS) is preferred as modifiers. The chemical properties of the modifier are systematically studied using infrared spectroscopy experiments. Anti-UV aging-modified asphalt is prepared and subjected to full cycle UV aging treatment using the durability test chamber. The influence of hindered amine light stabilizers on the basic properties of asphalt under UV aging conditions is analyzed. Scanning electron microscope and atomic force microscopy are used to deeply characterize the evolution law of micromorphology of modified asphalt during UV aging. The composition and variation of functional groups in UV-aged-modified asphalt are studied using the Fourier transform infrared spectroscopy system. The research results indicate that the addition of HALS could increase the penetration and ductility of asphalt and the increasing effect could reach 29 and 35%. When subjected to UV radiation, the maximum improving effect of HALS could reach above 50%. Hindered amine light stabilizers could react with asphalt materials and cause aromatization changes in asphalt components. The typical functional group indices of asphalt decreased by 90% approximately. Under the action of ultraviolet radiation, the modified asphalt could show good antiaging performance and could inhibit the aging behavior of the 70# asphalt and the deterioration of road performance.

Keywords: pavement, asphalt binder, aging resistance

1 Introduction

Asphalt is one type of core binder material in road construction, and its service life and performance are greatly influenced by environmental factors [1–3]. Particularly under prolonged exposure to ultraviolet (UV) radiation, oxygen, and high temperatures, asphalt undergoes significant aging [4]. The primary manifestations of asphalt aging include oxidation, loss of volatile components, increased viscosity, and enhanced brittleness [5,6]. These aging effects not only degrade the mechanical properties of the pavement but also lead to issues such as cracking and raveling, ultimately shortening the road's lifespan [7–9]. Therefore, a thorough understanding of the aging mechanisms in asphalt and the exploration of effective antiaging strategies are crucial for enhancing the durability of road materials.

Currently, the aging mechanisms of asphalt are primarily categorized into thermal-oxidative aging and photo-oxidative aging [10]. Thermal-oxidative aging occurs during the asphalt paving process and throughout its service life, as the sustained exposure to high temperatures and oxygen leads to the evaporation of lighter components in asphalt and the oxidation and crosslinking of its molecular structure, causing it to harden [11–13]. Photo-oxidative aging, on the other hand, is triggered by UV radiation from sunlight, which breaks asphalt's molecular chains, generating free radicals and accelerating the oxidation process [14,15]. While these aging mechanisms have been extensively studied, effectively mitigating aging in practical applications remains a significant challenge.

To address asphalt aging, the addition of antiaging modifiers has become a common approach [16]. These modifiers improve asphalt's antiaging properties by altering its chemical composition or physical structure [17]. Common

* **Corresponding author: Xiaolong Sun,** School of Civil Engineering and Transportation, Guangdong University of Technology, Guangzhou, 510006, China, e-mail: xls1998@gdut.edu.cn
Guanghui Zheng: Guangdong Provincial Government Loan Repayment Expressway Management Center, Guangzhou, 510199, China; School of Civil Engineering and Transportation, Guangzhou University, Guangzhou, 510006, China
Jingqing Liang, Xuehui Zheng: Guangdong Provincial Government Loan Repayment Expressway Management Center, Guangzhou, 510199, China
Hualong Xu: School of Civil Engineering and Transportation, Guangdong University of Technology, Guangzhou, 510006, China

modifiers include polymers, antioxidants, and UV-blocking agents [18,19]. However, despite the ability of existing modifiers to delay aging to some extent, they still have limitations [20]. For instance, some modifiers exhibit poor compatibility with asphalt, resulting in uneven distribution and, consequently, reduced effectiveness [21]. In addition, certain modifiers degrade under prolonged UV exposure, losing their functionality [22].

In recent years, the application of hindered amine light stabilizers (HALS) in asphalt pavement materials has garnered significant attention. HALS are known for their ability to capture free radicals and terminate free radical chain reactions, exhibiting excellent resistance to photo-oxidative aging [23]. This makes them particularly effective in inhibiting the aging process during extended UV exposure. Although HALS have been widely used in polymers and coatings, research on their application in asphalt materials is still in its early stages, and researchers are gradually accumulating empirical data on their performance and mechanisms of action. The antiaging mechanism of HALS was first proposed by Qian *et al.* [24], who demonstrated that under simulated UV aging conditions, HALS significantly slowed down oxidation reactions by scavenging peroxy radicals in asphalt, thereby extending the material's service life. In further studies, Li *et al.* [25] investigated the interaction between HALS and asphalt binders, finding that HALS not only substantially enhanced the photo-aging resistance of asphalt but also maintained its physical stability over a wide range of temperatures. This study highlighted that HALS exhibited good adaptability to various types of asphalt binders, particularly demonstrating superior stability in high-temperature environments. Wang *et al.* [26] evaluated the antiaging performance of HALS in regions with high temperatures and strong UV radiation through field tests and accelerated laboratory aging experiments. Their results showed that HALS effectively reduced the rate of asphalt hardening and decreased the amount of oxidative by-products. Chen *et al.* [27] further corroborated these findings, noting that the UV resistance of HALS could be optimized by adjusting dosage and dispersion techniques to address the photo-oxidative aging challenges posed by different climatic conditions. Regarding the synergistic effects of HALS with other antiaging modifiers, Chen *et al.* [28] found that combining HALS with UV-blocking agents produced synergistic effects, significantly extending the lifespan of asphalt under UV exposure. Moreover, this combination allowed for a reduction in the required amount of HALS, lowering costs while improving long-term durability. Chen *et al.* [29] investigated the synergistic effects between HALS and antioxidants, such as organotin compounds, demonstrating that the two acted through different mechanisms to concurrently inhibit thermal-oxidative and photo-oxidative aging, thereby enhancing asphalt's overall antiaging performance. These findings suggest that the combination of HALS with other antiaging agents offers more flexible solutions for the design of modified asphalt materials in the future. In terms of HALS performance in different asphalt matrices, Wang *et al.* [30] reported that HALS exhibited better dispersion and antiaging performance in highly polar asphalts, particularly in materials containing reclaimed asphalt pavement (RAP). Their study found that the interaction between HALS and highly polar binders enhanced stability, allowing HALS to provide continuous UV protection during the aging process. Zhang and Liu [31], through dynamic mechanical analysis (DMA), explored the microstructural changes in asphalt matrices modified with HALS, demonstrating that HALS formed a relatively uniform distribution network within the binder, thereby improving its antiaging capacity. Finally, Xu *et al.* [32] conducted long-term field experiments to evaluate the performance of HALS-modified asphalt in real-world road conditions. Their results indicated that HALS outperformed conventional antiaging agents in high-temperature, high-humidity environments, particularly on road surfaces exposed to strong UV radiation, where it significantly reduced the frequency of cracking and raveling. However, the study also noted that over time, the antiaging effects of HALS might diminish due to environmental degradation, suggesting that its long-term stability under extreme climate conditions requires further investigation. While the application and performance of HALS in asphalt have been largely validated, the precise mechanisms of HALS in asphalt and the factors influencing its effectiveness remain unclear, potentially hindering the broader adoption of HALS in controlling UV-induced aging of asphalt.

Therefore, the hindered amine light stabilizer is preferred as modifiers in this study. The chemical properties of the modifier are systematically studied. Anti-UV aging-modified asphalt is prepared and subjected to full cycle UV aging treatment. The influence of hindered amine light stabilizers on the basic properties of asphalt under UV aging conditions is analyzed. The evolution law of micromorphology of modified asphalt during UV aging are deeply characterized. The composition and variation of functional groups in UV-aged-modified asphalt are studied, which will provide relevant basis for improving the antiaging performance of asphalt pavement materials.

2 Materials and methodology

2.1 Materials

2.1.1 Modifier

Based on the good antiaging performance of light stabilizer in polymer materials, Tinuvin770 hindered amine light stabilizer (T770) was selected as the modifier to prepare modified asphalt. The molecular formula of T770 is $C_{28}H_{52}O_4N_2$, and molecular weight is 480.7. The application dosage range of light stabilizers in asphalt is 0.2–0.8%.

2.1.2 Asphalt

70# asphalt was selected as the 70# asphalt for the preparation of modified asphalt. According to the "Test Specification for Asphalt and Asphalt Mixtures in Highway Engineering" (JTG E20-2019), 70# asphalt was subjected to technical performance testing. The specific technical performance index values of 70# asphalt are presented in Table 1.

2.1.3 Preparation of modified asphalt

The process flow of preparing antiaging-modified asphalt with hindered amine light stabilizer is as follows: First, 70# asphalt is put into the oven at 135°C for 1.5 h. The flowing asphalt is poured into a clean beaker and placed on the oil bath heating device at 160 ± 5°C for insulation. Hindered amine light stabilizers of the mass fraction of 0.2–0.8% asphalt weight were added into the asphalt and stirred at the shear rate of 5,000 rad·min^{-1} for 5 min. The prepared light stabilizer-modified asphalt was placed in the oven at 115°C to swell. After the swelling is completed, the light stabilizer-modified asphalt is obtained.

2.2 Methodology

2.2.1 UV aging test

The UV weatherability test chamber was selected as the test equipment in this article. The UV radiation output power of the test equipment is 300 W, and the radiation area is 0.8 m^2, whose UV radiation density could be calculated as 375 W·m^{-2}. According to the radiation conditions in high altitude areas (such as Tibet in China), the average annual solar radiation intensity is about 7,000 MJ·m^{-2}·a. According to the proportion of ultraviolet radiation intensity from 5% to 6%, the annual average outdoor ultraviolet radiation intensity could be calculated to be about 7,000 MJ·m^{-2}·a *6% = 420 MJ·m^{-2}·a. The radiation output intensity of indoor ultraviolet aging light source is about 375 W·m^{-2}. According to the calculation method of indoor simulation time = total natural ultraviolet radiation/indoor simulated ultraviolet intensity, the indoor simulation time is $420 \times 10^6/375 = 1.1 \times 10^6$s ≈ 305 h, equal to 1 year in natural environment of Tibet of China. The accelerated UV aging time nodes are set at 76.25, 152.5, 228, and 305 h.

Table 1: Technical performance indicators of 70# asphalt

Test	Results	Requirement
Penetration/0.1 mm	62.8	60–80
15°C Ductility/cm	>100	>100
Softening point/°C	47.6	≥45
Solubility/%	99.7	≥99.5
Wax content/%	2.0	≤2.2

2.2.2 XRD

The chemical structure of hindered amine light stabilizer is characterized by German Bruker D8 ADVANCE X-ray diffractometer (XRD) to obtain its molecular solid structure information. The experimental scanning angle range is 1.5°~60°, the scanning rate is 5°/min, and the step size is 0.02°.

2.2.3 Fourier transform infrared spectroscopy (FTIR)

The TG 209 F1 thermogravimetric infrared spectroscopy system produced by NETZSCH in Germany is used to analyze the functional group composition changes of light stabilizer-modified asphalt. The experimental scanning frequency is 32 times, with the resolution of 4 cm^{-1}. The experiment is conducted in the nitrogen atmosphere, with nitrogen as the reaction gas. The blowing flow rate is 50 mL·min^{-1}, the heating rate is 10°C·min^{-1}, and the test temperature range is from 30 to 500°C.

2.2.4 Physical performance

According to the "Test Specification for Asphalt and Asphalt Mixtures in Highway Engineering" (JTG E20-2019) T0604-2011, the penetration test is conducted on modified asphalt at 25°C and the penetration time is 5 s. According to T0605-2011, the ductility test is conducted at the temperature of 15°C and the stretching speed of 5 cm·min^{-1}. According to T0606-2011, the softening point test is conducted with the initial temperature of 5°C and the heating rate is 5°C·min^{-1}.

2.2.5 Rheological property

Rheological tests on the asphalt were conducted using a strain-controlled mode, with a controlled strain of 12% and a test frequency of 10 rad·s^{-1}. A parallel plate configuration with the diameter of 25 mm and a gap of 1 mm was employed. The test temperature ranged from 46 to 82°C, with 6°C increments. At each set temperature, the sample was conditioned for 10 min. The complex shear modulus and phase angle were recorded every 2 min, with five data points collected at each temperature setting, and the average value was calculated.

2.2.6 Scanning electron microscope (SEM)

SEM analysis is conducted using the JSM-IT100 scanning electron microscope produced by JEOL Company in Japan. The test adopts the acceleration voltage of 5KV and the amplification factor of 200–1,000. Before SEM analysis, the asphalt specimens are subjected to the 90 s surface spray gold treatment.

2.2.7 Atomic forces microscope (AFM)

Dimension FastScan Scanning probe microscopy produced by Bruker Company is used to characterize the change of surface roughness of ultraviolet aging-modified asphalt. The fast scanning probe is used for testing, scanning the micromorphology of the sample surface in ScanAsyst intelligent mode. The probe of the instrument used is the silicon nitride cantilever probe. The scanning range of view is 80 μm × 80 μm. The testing flowchart of this study is shown in Figure 1.

3 Results and discussion

3.1 Chemical composition of modifier

The dynamic FTIR test results of T770 light stabilizer are shown in Figure 2. From the analysis in Figure 2, it could be seen that there is almost no substance escaping from the T770 light stabilizer in the first 30 min, and its intensity is relatively stable. At the end of this period, the curve showed the certain degree of increase, indicating that as the temperature gradually increased, the connection strength between some unstable structures in T770 light stabilizer and the main body deteriorates. The small protrusions that appeared at 36.09 min might be due to the mixing of impurities such as carbon dioxide causing the change in intensity, which could be seen in the infrared spectrum as a weak peak at 1,500 cm^{-1}. A strong characteristic peak formed by the antisymmetric stretching vibration of methylene and the C–H vibration absorption peak of olefins at 1454.39 and 1375.66 cm^{-1} are observed in the infrared spectrum corresponding to 2929.37 cm^{-1}. With the change of temperature (time), the reaction rate of T770 light stabilizer reaches its maximum and then rapidly decreases. At 50.05 min, the infrared spectrum curve tends to flatten out, and the intensity of the characteristic peaks is also weakened, but there is no significant change in the position of the characteristic peaks.

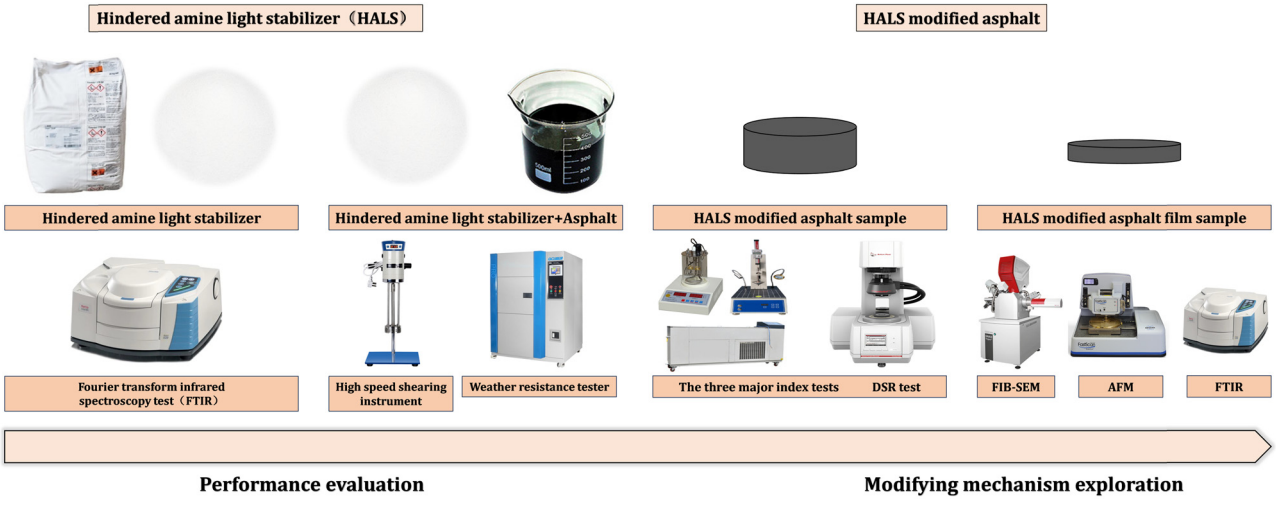

Figure 1: Testing flowchart.

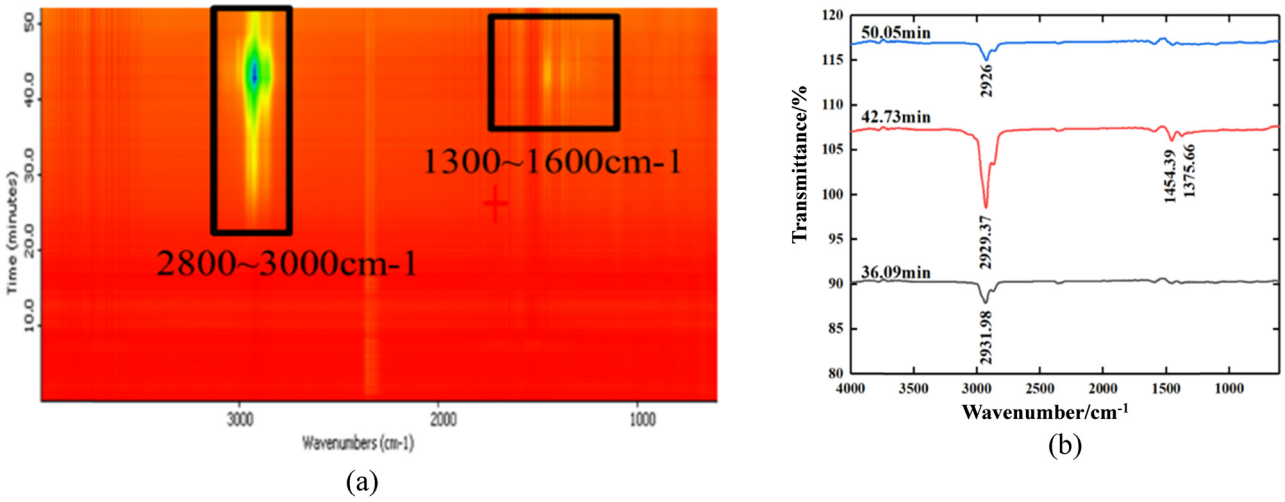

Figure 2: Infrared spectral analysis results: (a) 2D spectrogram and (b) FTIR spectrogram.

3.2 Physical performance of modified asphalt

The basic properties of 70# asphalt and T770-modified asphalt under different UV aging times are shown in Figure 3. From the analysis shown in Figure 3(0%), it could be seen that with the extension of UV aging time, the penetration of 70# asphalt shows the significant downward trend, indicating that UV radiation could cause the increase in asphalt hardness. The softening point of matrix asphalt

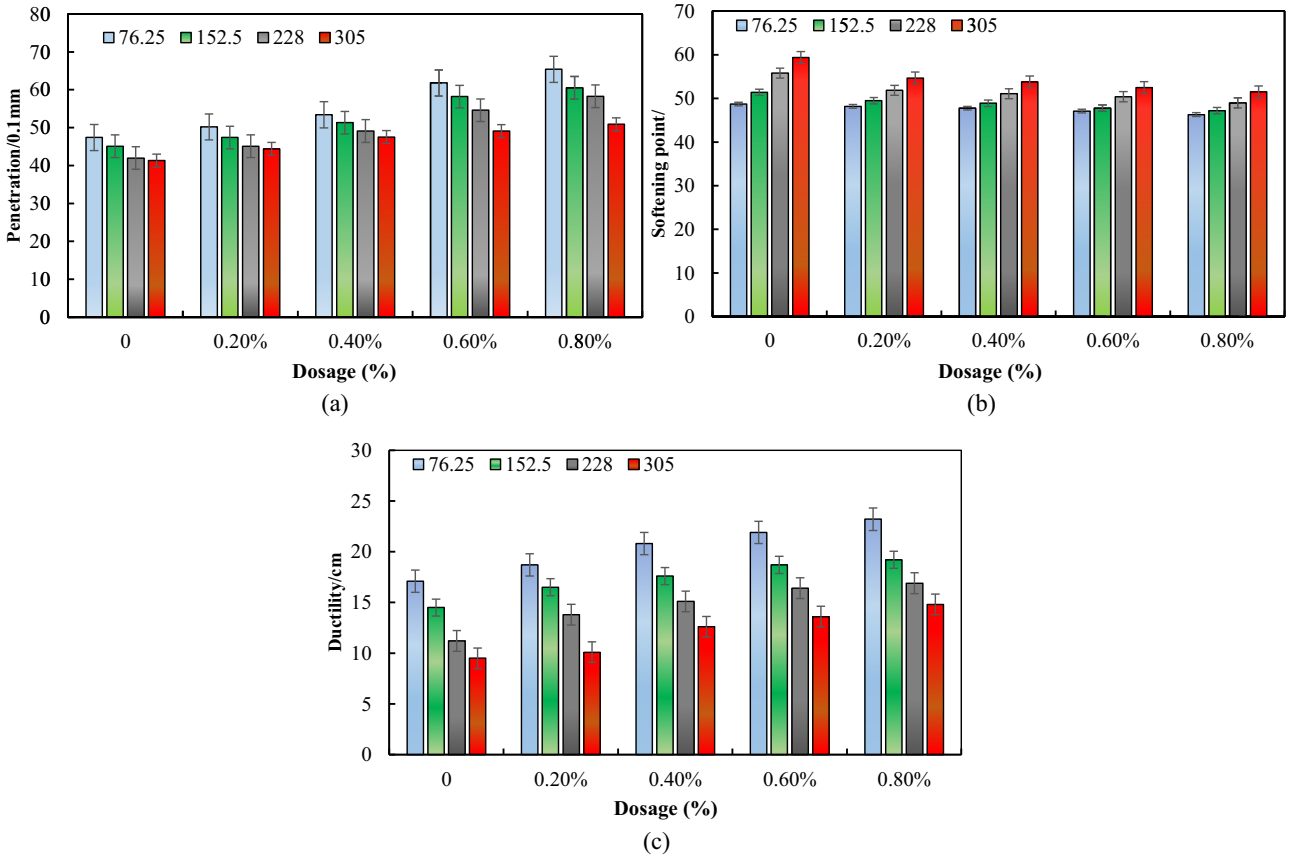

Figure 3: Physical performance of UV-aged 70# asphalt (0%) and T770-modified asphalt: (a) penetration, (b) softening point, and (c) ductility.

significantly increases with the extension of UV aging time, mainly due to the increase of heavy components in asphalt, which leads to the increase in asphalt viscosity. The ductility of 70# asphalt showed the significant decrease with the UV aging process, which is directly related to the hardening of the asphalt texture and is basically consistent with the change pattern of penetration. In summary, UV aging could lead to the hardening of asphalt texture, manifested in the increase in softening point and the significant decrease in penetration and ductility at the performance level.

From the analysis shown in Figure 3, it could be seen that with the extension of UV aging time, the penetration of T770-modified asphalt shows the significant downward trend under different modifier dosages, indicating that UV radiation could cause aging of asphalt material and directly increase its hardness. Under the determined UV aging time, the penetration of modified asphalt would gradually increase with the rise of T770 modifier dosage. Compared with the unaged modified asphalt, the penetration reduction of T770-modified asphalt with the 0.4% dosage is the smallest, specifically 2.07 mm, while the penetration reduction of T770-modified asphalt with the maximum dosage (modifier content of 0.8%) is the largest, reaching about 3 mm. This indicates that the UV aging control effect of T770 light stabilizer has the optimal value, and continuous increase in modifier dosage might cause the decrease in the basic performance of asphalt during UV aging.

From the analysis of the trend of changes in ductility and softening point, it could be seen that the extension of UV aging time would cause the decrease in the ductility of modified asphalt. However, with the increase of dosage, the ductility gradually increases, indicating that the

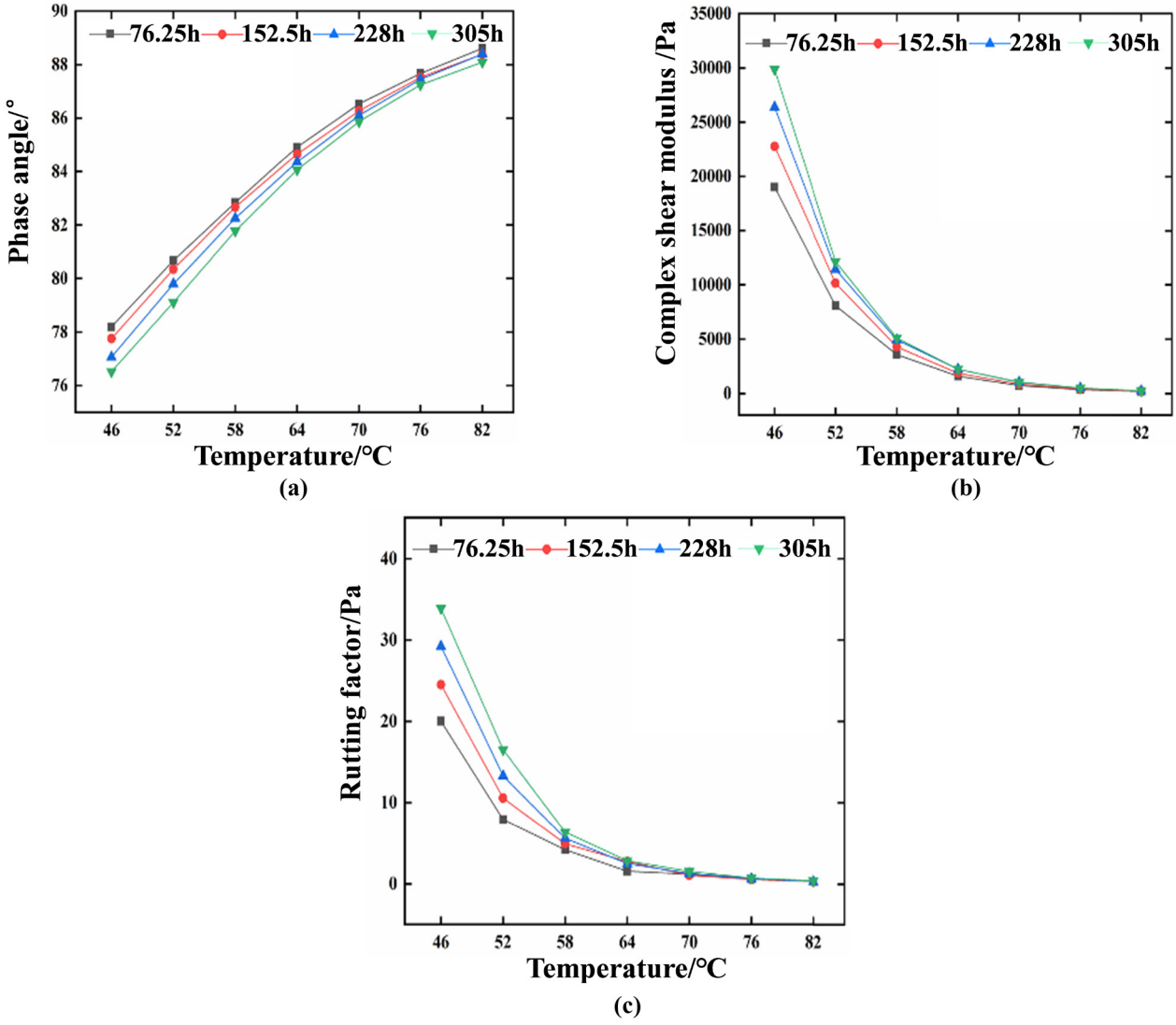

Figure 4: Rheological performance of UV-aged 70# asphalt: (a) phase angle, (b) complex shear modulus, and (c) rutting factor.

addition of T770 light stabilizer could effectively suppress the deterioration of ductility. It is worth noting that with the increase of T770 modifier dosage, the change rate in ductility of modified asphalt gradually decreases, which proves that T770 modifier has good UV radiation resistance. According to the comparative analysis of softening point, it could be seen that the softening point increases with the increase of aging time. As the dosage increases, the softening point decreases with the increase of aging time, indicating that ultraviolet radiation improves the high-temperature stability of asphalt, while high dosage of T770 light stabilizer improves the UV radiation resistance of asphalt binder.

3.3 Rheological performance of modified asphalt

Figures 4(a) and 5(a) present the temperature sweep test results (phase angle) for the 70# base asphalt and T770-modified asphalt, respectively. The analysis of Figures 4(a) and 5(a) reveals that the phase angle for both types of asphalt increases with temperature, indicating that higher temperatures lead to increased viscosity and decreased elasticity of the asphalt. Additionally, as the ultraviolet aging time increases, the phase angle of both the 70# base asphalt and the antiaging-modified asphalt decreases significantly, suggesting that ultraviolet

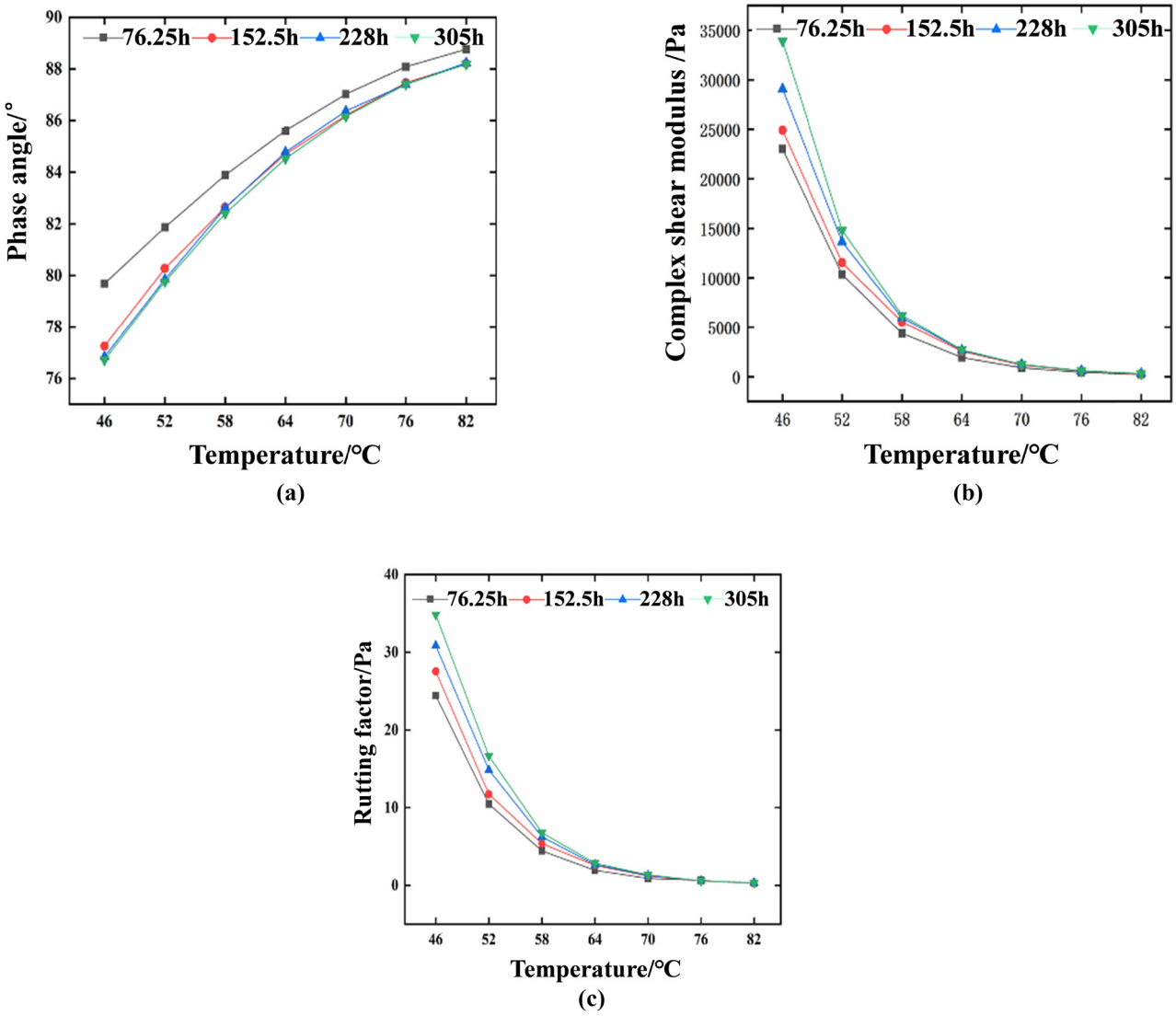

Figure 5: Rheological performance of UV-aged T770-modified asphalt: (a) phase angle, (b) complex shear modulus, and (c) rutting factor.

radiation enhances the elastic response of the asphalt. Furthermore, this effect becomes more pronounced with longer radiation exposure. Notably, the reduction in phase angle with increasing ultraviolet exposure is less pronounced for the antiaging-modified asphalt compared to the base asphalt, indicating that the T770 light stabilizer effectively enhances the ultraviolet aging resistance of the asphalt binder to some extent.

Figures 4(b) and 5(b) show the complex modulus results from the temperature sweep tests for the 70# base asphalt and T770-modified asphalt. From the analysis of Figures 4(b) and 5(b), it is evident that the complex modulus of both types of asphalt decreases gradually with the increasing temperature. As the ultraviolet aging time increases, the complex modulus of the asphalt shows a significant increase, suggesting that ultraviolet radiation induces hardening of the asphalt binder, enhancing its resistance to deformation. A comparison with the base asphalt shows that the increase in complex modulus for T770-modified asphalt is less pronounced, which confirms the good ultraviolet aging resistance of the T770 modifier and its ability to mitigate significant changes in the modulus caused by ultraviolet radiation. Furthermore, when the ultraviolet aging time is within the range of 76.25 to

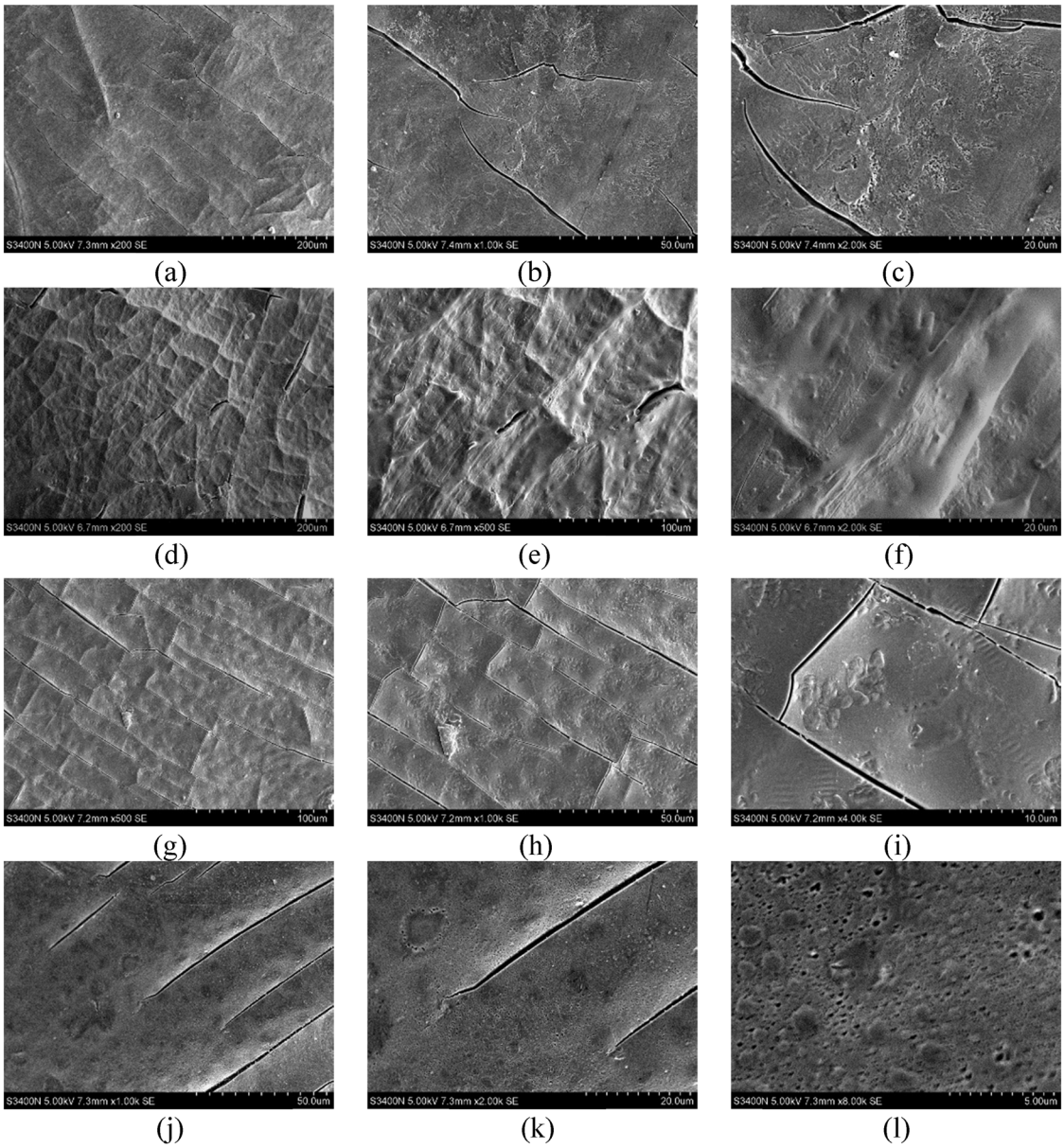

Figure 6: Ultraviolet-induced microscopic morphology of 70# asphalt. (a) 76.25 h-200 μm, (b) 76.25 h-100 μm, (c) 76.25 h-20 μm, (d) 152.5 h-200 μm, (e) 152.5 h-100 μm, (f) 152.5 h-20 μm, (g) 228h-200 μm, (h) 228 h-100 μm, (i) 228 h-10 μm, (j) 305 h-100 μm, (k) 305 h-50 μm, and (l) 305 h-10 μm.

152.5 h, the difference in complex modulus between T770 and T622-modified asphalts is relatively small. As the ultraviolet exposure time increases, the difference in complex modulus of T770-modified asphalt becomes more apparent, with a significant increase in hardness, indicating that, during the early stages of ultraviolet radiation, its effect on the asphalt's resistance to deformation is not significant. However, as the exposure time continues to extend, the effect becomes more pronounced, leading to a substantial increase in the hardness of the asphalt binder.

Figures 4(c) and 5(c) present the rutting factor results from the temperature sweep tests for the 70# base asphalt and T770-modified asphalt. Analysis of Figures 4(c) and 5(c) shows that the change in the rutting factor follows a similar trend to the complex modulus, gradually decreasing with the increasing temperature. This suggests that ultraviolet radiation improves the asphalt's resistance to deformation under high-temperature conditions, and this enhancement becomes more pronounced with longer ultraviolet aging. It is noteworthy that, compared to the base asphalt, the difference in rutting factor for T770-modified asphalt between 76.25 and 152.5 h of ultraviolet aging is not significant. With further extension of the ultraviolet aging time, the change in the rutting factor for T770-modified asphalt becomes relatively smaller, indicating that the hindered amine light stabilizer can improve the ultraviolet aging resistance of the asphalt binder.

3.4 Microscopic morphology analysis based on UV aging

3.4.1 SEM analysis

3.4.1.1 70# asphalt

Figures 6 and 7 shows the characterization results of the UV-induced microstructure of 70# asphalt with different scanning times. From Figures 6 and 7, it can be observed that after 76.25 h of UV aging, there are obvious aggregated parallel cracks on the surface of the matrix asphalt, and there are locally closed fracture areas. When the UV aging time is extended to 152.5 h, a series of closed blocks appear on the asphalt surface, and there is a clear shared boundary between the blocks. When the UV aging time reached 228 h, dense parallel cracks appears again on the asphalt surface, and vertical cracks intersecting with parallel cracks also are presented, which causes the parallel cracks to connect with each other and leads to the appearance of closed cracks and blocky fragments. When the UV aging time reaches 305 h, the

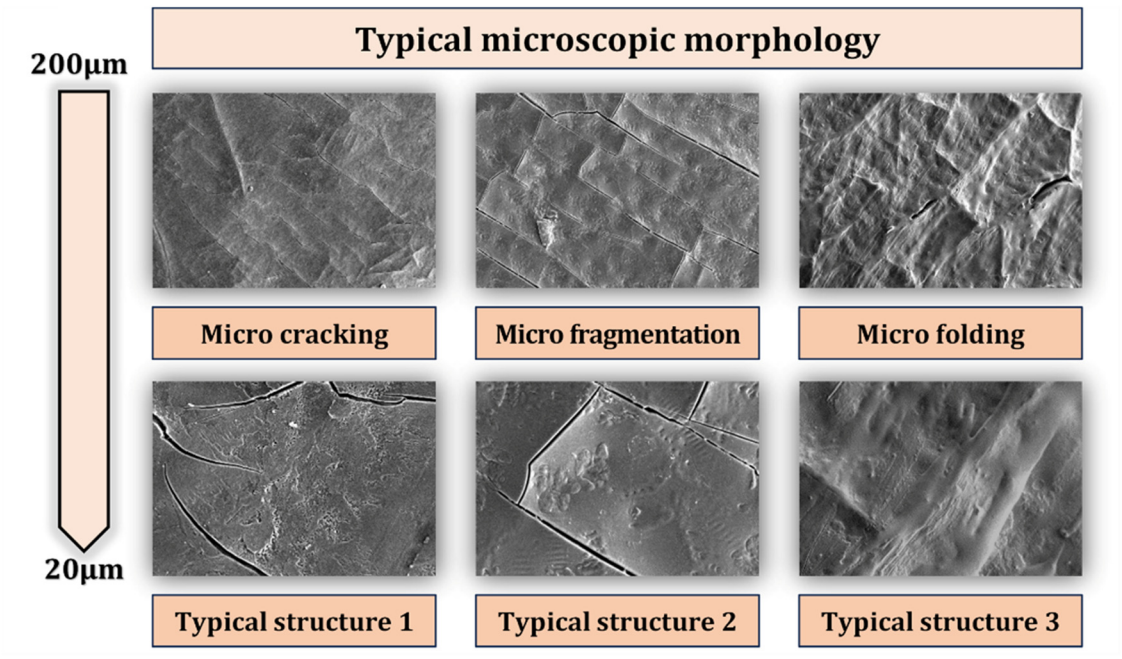

Figure 7: Typical microscopic morphology of 70# asphalt.

closed cracks on the asphalt surface disappear and mainly appear as parallel cracks, while the density and the number of cracks significantly decrease.

3.4.1.2 Modified asphalt

The UV-induced microstructure of T770-modified asphalt is shown in Figures 8 and 9. From Figures 8 and 9, it could be analyzed that after 76.25 h of UV aging, high-density microcracks appeared on the surface of T770-modified asphalt, and the microcracks are basically interconnected, forming fragments composed of closed cracks. The UV aging time continues to extend to 152.5 h, and the network structure composed of closed fragments could still be recognized on the surface of T770-modified asphalt. The regional boundaries of each closed fragment structure are no longer obvious, and boundary cracks have disappeared. After 228 h of UV aging, the microstructure of T770-modified asphalt changes again, and the boundary fuzzy closed fragment structure disappears. The protruding structure transforms into a distinct fold structure, and the area between the folds has good flatness. When the UV aging time continues to extend to 305 h, the density of the fold structure increases, but no obvious closed microstructure is formed.

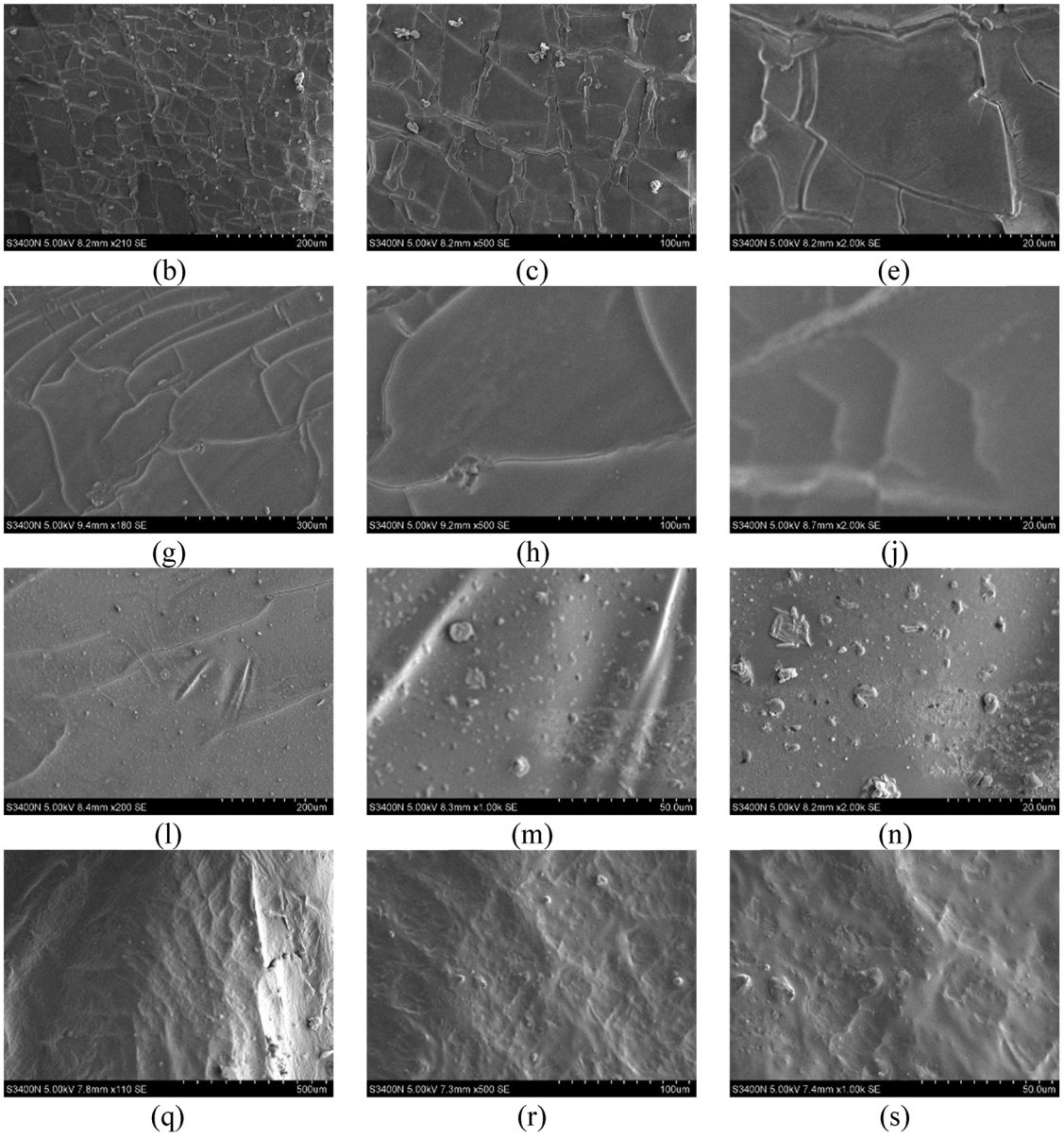

Figure 8: Ultraviolet-induced microscopic morphology of modified asphalt. (b) 76.25 h-200 μm, (c) 76.25 h-100 μm, (e) 76.25 h-20 μm, (g) 152.5 h-200 μm, (h) 152.5 h-100 μm, (j) 152.5 h-20 μm, (l) 228 h-200 μm, (m) 228 h-50 μm, (n) 228 h-20 μm, (q) 305 h-200 μm, (r) 305 h-100 μm, and (s) 305 h-50 μm.

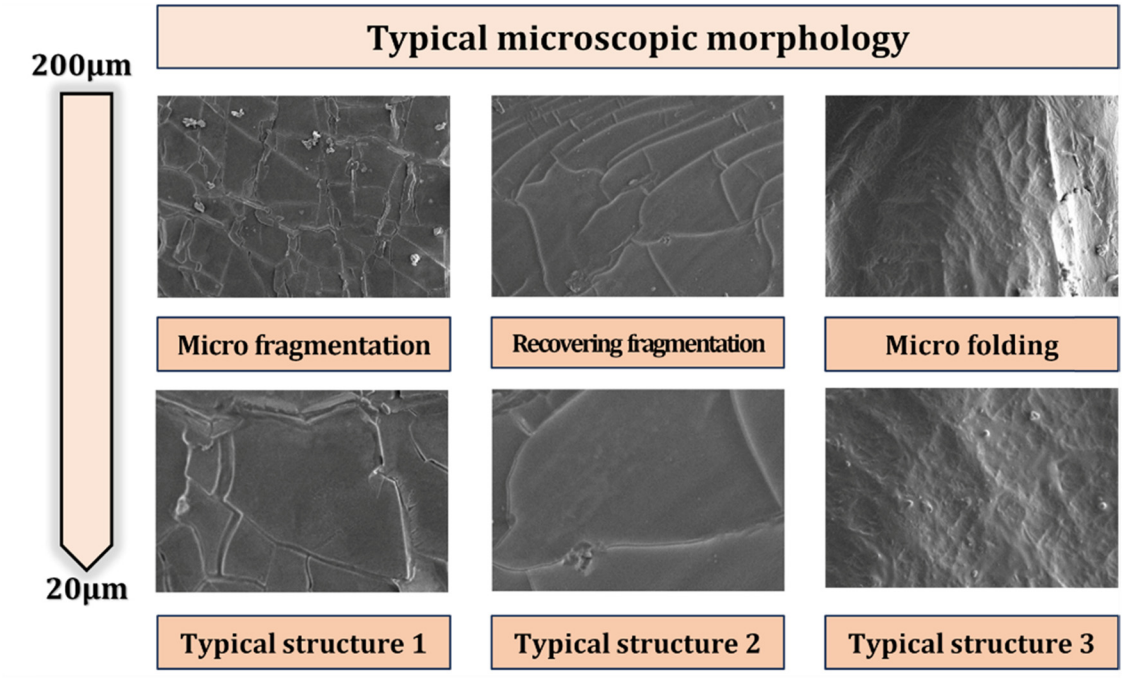

Figure 9: Typical microscopic morphology of modified asphalt.

3.4.2 AFM analysis

3.4.2.1 70# asphalt

Figure 10 shows the AFM characterization results of matrix asphalt under different UV aging time conditions. The distribution of bright and dark domains in the figure shows the clear boundary of aggregation regions, indicating that as the UV aging process progresses, the overall morphology of asphalt gradually becomes more complex. As the UV aging time continues to extend, the distribution

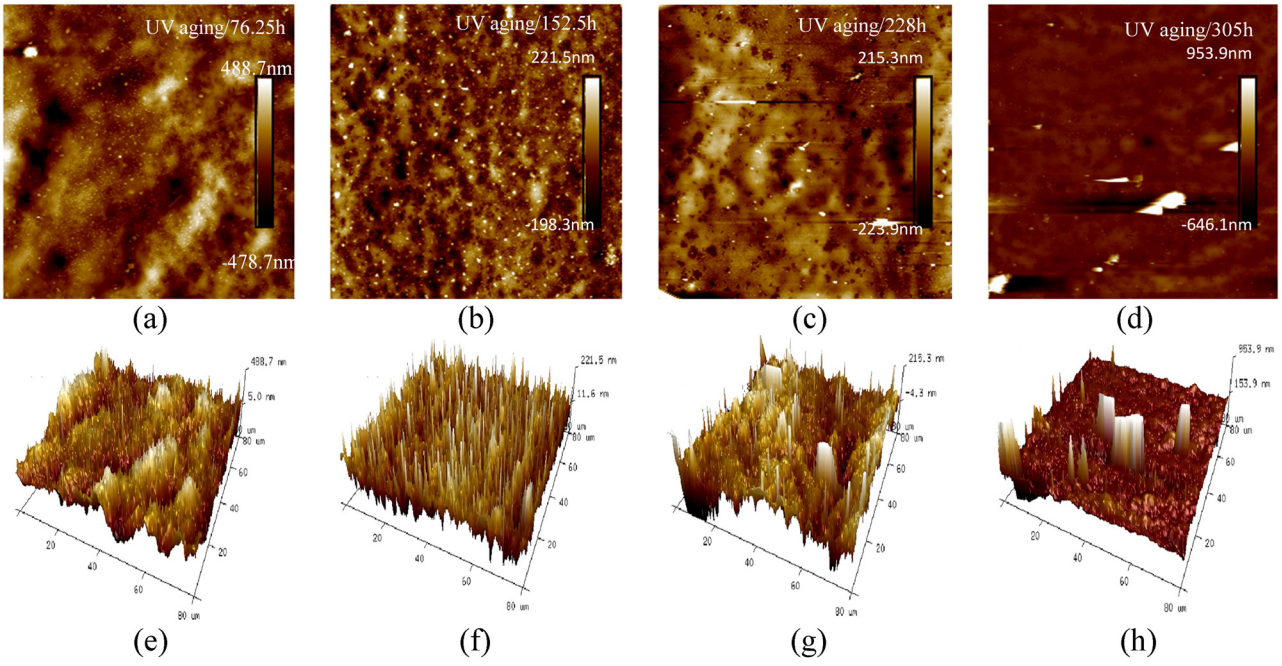

Figure 10: AFM results of 70# asphalt under different UV aging times. (a) 76.25 h-2D. (b) 152.5 h-2D. (c) 228 h-2D. (d) 305-2D. (e) 76.25 h-3D. (f) 152.5 h-3D. (g) 228 h-3D. (h) 305-3D.

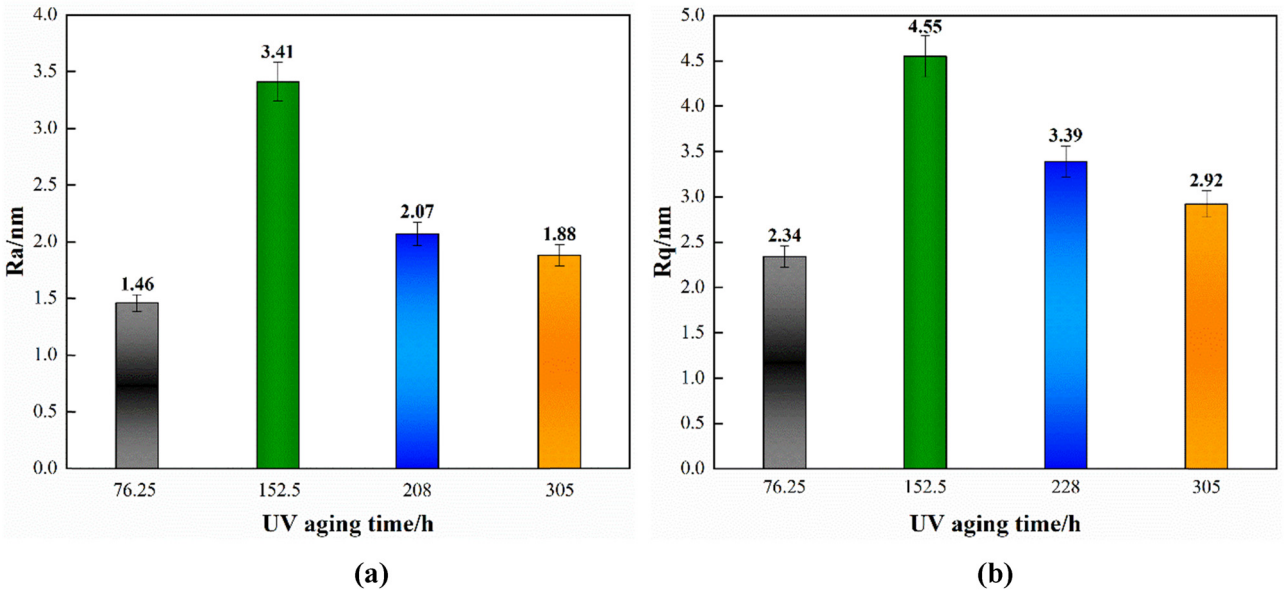

Figure 11: Roughness R_a and R_q of 70# asphalt under different UV aging times. (a) R_a and (b) R_q.

of bright regions gradually concentrates, and the boundary between bright and dark regions in the figure becomes more obvious. In the 3D analysis results, the changes in surface morphology are more significant. The total height of the aged matrix asphalt surface in the figure decreases, manifested as the uniformly distributed "needle like structure" in the 3D morphology image. When the aging time is 228 h, the area of the bright region begins to concentrate, and the large diameter aggregated "columnar structure" appears in the figure. When the UV aging time reaches 305 h, the bright regions in the image are highly concentrated, and there is the clear aggregation convex structure on the surface of the matrix asphalt in the 3D morphology image. Figure 11 shows the roughness R_a and R_q of 70# asphalt under different UV aging times. Figure 11 shows that the roughness of 70# asphalt increased first and

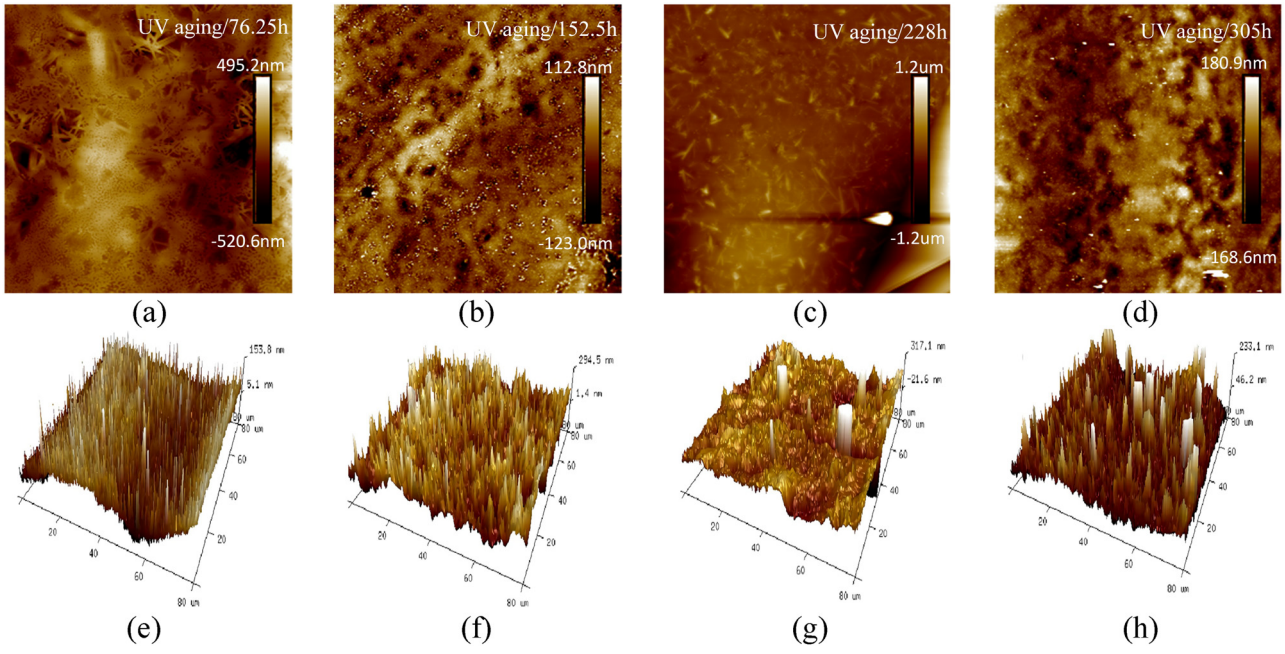

Figure 12: AFM results of the modified asphalt under different UV aging times. (a) 76.25 h-2D, (b) 152.5 h-2D, (c) 228 h-2D, (d) 305-2D, (e) 76.25 h-3D, (f) 152.5 h-3D, (g) 228 h-3D, and (h) 305-3D.

then decreased. The roughness of the film reached the maximum and then decreased obviously, which was consistent with the results reflected from the AFM graph.

3.4.2.2 Modified asphalt

Figure 12 shows the AFM-2D and 3D characterization results of T770-modified asphalt under different UV aging times. When the UV aging time is extended to 76.25 h, the area of bright spots and dark areas in the figure increase, resulting in the "needle like structure." This is similar to the microstructure of the matrix asphalt with the same aging time, but the surface fluctuation of T770-modified asphalt is smaller. This might be due to the fact that T770 modifier in modified asphalt could inhibit the oxidation and condensation of light components, especially aromatic components, reducing the loss of light components, thereby maintaining the relatively flat microsurface morphology. When the UV aging time is 228 h, the bright areas on the asphalt surface are significantly concentrated, the height of the protruding structures is significantly reduced, which are interconnected to form closed and irregular shapes. This might be due to the coupling effect of UV and temperature, which leads to the photooxidation reaction of asphalt, the volatilization of light components, and the aggregation of heavy components, resulting in uneven distribution of components on the asphalt surface. When the UV aging time reaches 305 h, the large number of protruding structures are distributed on the asphalt surface. Based on the 3D characterization results, it could be seen that this protruding structure appears as the "columnar structure," and the dark region area significantly increases. However, the aggregation and the distribution of columnar structures on the modified asphalt surface are relatively average. Figure 13 shows the roughness R_a and R_q of modified asphalt under different UV aging times. From Figure 13, it could be concluded that the variation of roughness of the modified asphalt was same with that of 70# asphalt. However, the roughness values of 70# asphalt and modified asphalt were different. The roughness value of the modified asphalt was obviously smaller than that of 70# asphalt, which might supposed that the effect of T770 mitigates the surface variation of asphalt during UV aging process.

3.4.2.3 Comparison analysis

Figure 14 presents a comparison of the roughness between the 70# base asphalt and T770-modified asphalt. As shown in Figure 14, the surface roughness trend of the T770-modified asphalt is generally consistent with that of the 70# base asphalt; however, the specific values of R_a and R_q are relatively lower. This may be attributed to the inhibitory effect of the T770 light stabilizer on the aging behavior of asphalt, which is reflected in the reduction of surface roughness. As the ultraviolet aging time increases, the asphalt surface roughness first increases, then decreases, and finally stabilizes. This behavior is somewhat related to the appearance, development, and healing of microcracks observed in the SEM test results, and future research will focus on exploring this relationship.

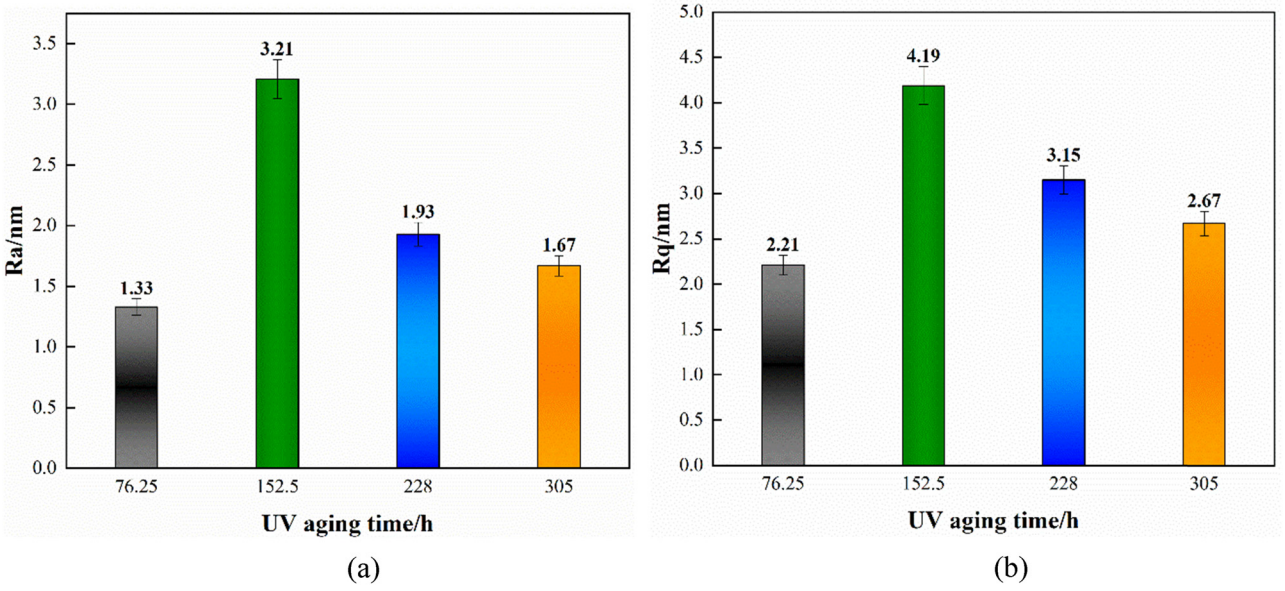

Figure 13: Roughness R_a and R_q of the modified asphalt under different UV aging times: (a) R_a and (b) R_q.

3.5 Analysis of changes in functional groups under UV aging

3.5.1 Analysis of functional group composition

3.5.1.1 70# asphalt

The specific test results of the functional group composition of 70# asphalt are shown in Figure 15. From Figure 15, it could be seen that the strong absorption peaks generated by 70# asphalt under ultraviolet light are all within the range of 2,800–3,000 cm^{-1}, and the absorption peaks in this range are mainly caused by the stretching vibration peaks of methylene and methyl. In addition, there are intermediate strength carbonyl functional groups at the wave number position of 1,700 cm^{-1}, which are generated due to the reaction of the internal components of the asphalt caused by the increase in temperature during the experiment. As the temperature rises, the reaction rate of the matrix asphalt also changes accordingly. The extension of UV aging time is not significantly related to the time when the matrix asphalt product begins to form, but corresponds to the temperature at which it reaches its peak. As the UV aging time increases, the peak temperature gradually increases, but the growth is relatively slow, with the entire time point only increasing by 10°C. Under prolonged ultraviolet radiation for 228 and 305 h, the absorption peak intensity in the region increased at around 1,500 cm^{-1}, indicating the significant difference in the functional groups generated during this time period compared to before. This might be due to the deepening of ultraviolet aging of asphalt binder.

3.5.1.2 Modified asphalt

It could be analyzed from Figure 16 that the characteristic peak positions of T770-modified asphalt under different UV aging times are basically consistent. The intensity of the gas generated at the initial temperature in the spectrum is relatively weak, mainly caused by the release of small molecule gases and the evaporation of water. The infrared spectra of T770-modified asphalt under four different UV aging times shows absorption peak regions with lower intensity and a certain width in the range of 3,700–3,800 cm^{-1}. At 2,930 cm^{-1}, an extremely strong absorption peak, as well as a characteristic peak with a shoulder peak of 2,870 cm^{-1} and a decreasing intensity of 1,455 and 1,377 cm^{-1}, were observed, specifically $-CH_2$ stretching vibration, symmetric stretching vibration of methylene CH_{2-}, and bending vibration of $CH_2(CH_3)$. The moderate intensity absorption peaks at 2,350 and 660 cm^{-1} represent CO_2 generated by the cleavage and recombination of hydroxyl and carboxyl compounds. According to the infrared spectrum analysis of T770-modified asphalt, the selected initial temperature gradually increases (267–363°C), and the production of modified asphalt products lags behind after aging treatment. After prolonged UV aging for 305 h, the initial temperature of the modified asphalt decreases. Among all the characteristic peak

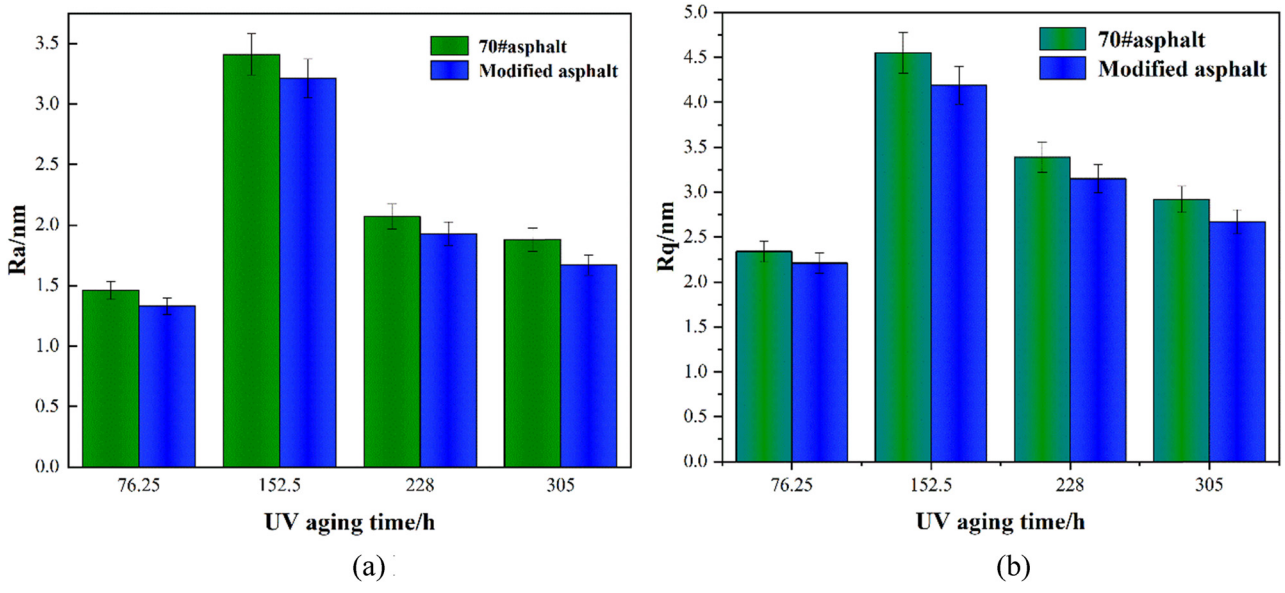

Figure 14: Roughness R_a and R_q comparison of UV-aged 70# asphalt and modified asphalt: (a) R_a and (b) R_q.

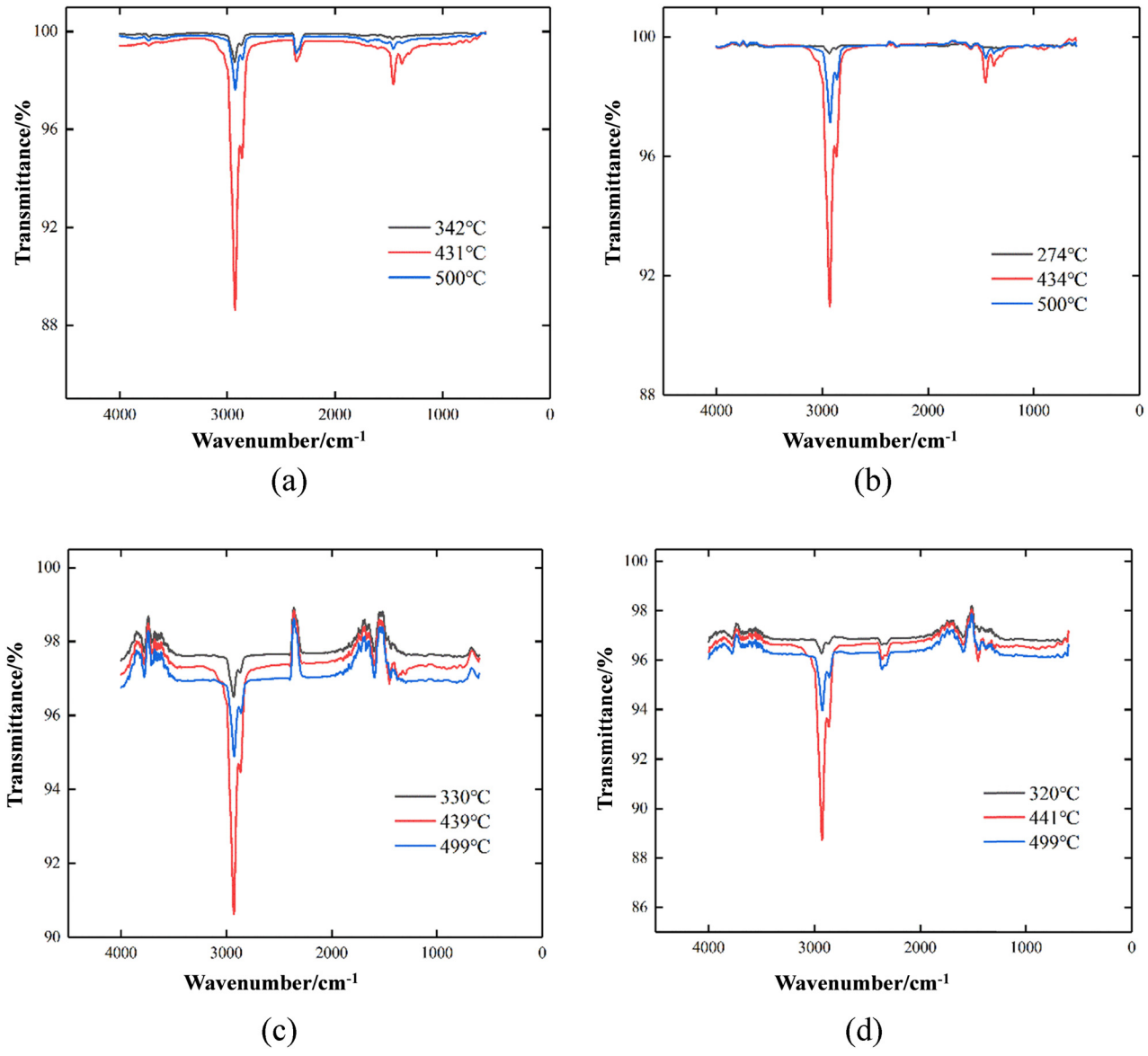

Figure 15: Infrared spectra of 70 # matrix asphalt under different UV aging times. (a) FTIR76.25 h, (b) FTIR-152.5 h, (c) FTIR-228 h, and (d) FTIR-305 h.

positions that appear, only the absorption peak intensity of about 2,930 cm^{-1} changes significantly with the increase of pyrolysis temperature. The characteristic peak at this position before 431°C rapidly decreases with the increase of temperature, reaching the lowest value of transmittance at 431°C. At this time, the gas intensity decomposed by asphalt at high temperature reaches the highest, and the absorption vibration peak of methylene at this position generates long-chain alkanes. The temperature difference corresponding to the highest peak of T770-modified asphalt under the other three UV aging times is only 5°C. The temperature corresponding to the highest peak of modified asphalt at 478°C indicates that after aging for 228 h, the impact on asphalt is relatively greatest, promoting the migration and transformation of internal heavy components of asphalt, resulting in the later production of asphalt products.

3.5.2 Functional group index analysis

3.5.2.1 70# asphalt

Due to the differences in the spectra between 70# asphalt and modified asphalt after aging, it is necessary to redefine the quantitative calculation formula for the spectra of 70# 70# asphalt. The index $\sum A$ is defined as follows:

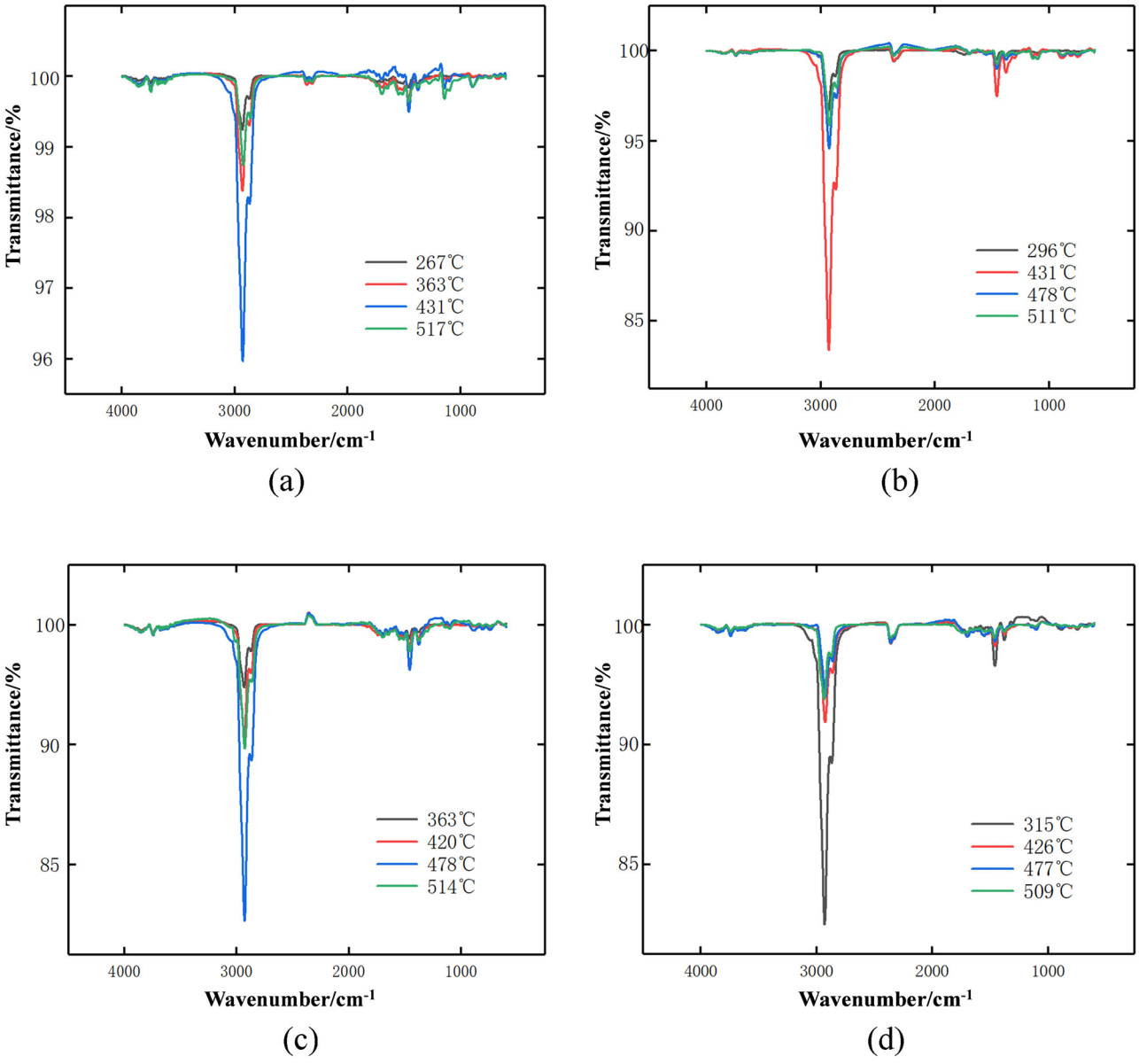

Figure 16: Infrared spectra of modified asphalt under different UV aging times. (a) FTIR76.25 h, (b) FTIR-152.5 h, (c) FTIR-228 h, and (d) FTIR-305 h.

$$\sum A = A_{1,700} + A_{1,601} + A_{1,456} + A_{1,377} + A_{1,300} + A_{1,030} + A_{902} + A_{746}. \quad (1)$$

According to Figure 17, under the action of ultraviolet radiation from 228 to 305 h, the aging degree of the matrix asphalt without the addition of modifier is significantly greater than the first two time points. The exponential growth of functional groups at the beginning and end time points of UV aging were 7.82 times of carbonyl group, 8.07 times of sulfoxide group, and 5.94 times of aromatic functional groups. The exponential growth of carbonyl group and sulfoxide group increases significantly, indicating that the matrix asphalt suffers from obvious aging after a long time of ultraviolet radiation, and the ultraviolet aging destroys the colloidal structure stability of asphalt.

3.5.2.2 Modified asphalt

The functional group index caused by the aging process is calculated, and the characteristic peak area calculation method is selected. The wavenumber range of 2,000–650 cm^{-1} in the fingerprint area is selected as the standard for quantitative analysis of FTIR spectra. This article selects the position with the highest absorbance and wavenumber from four UV aging time points as the

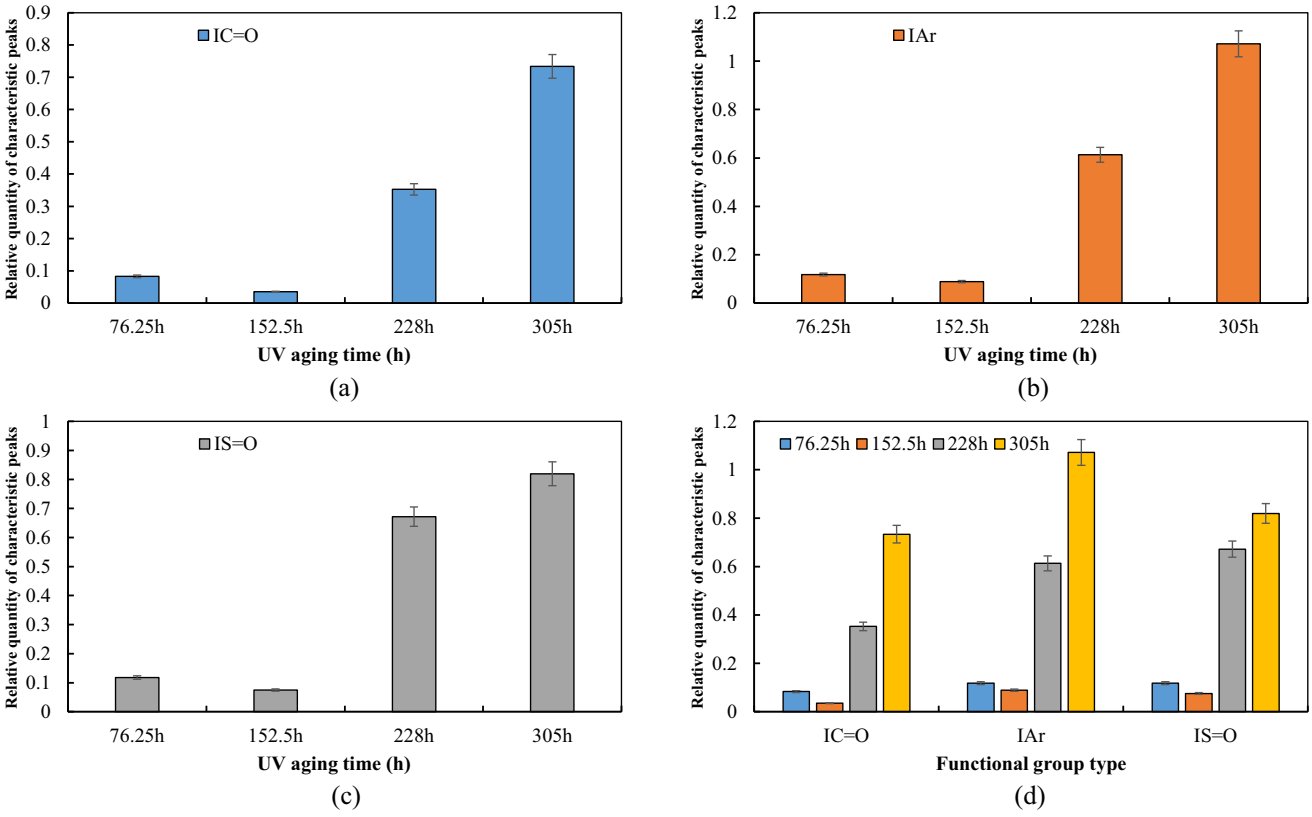

Figure 17: Characteristic functional group index of 70# asphalt under different aging times: (a) carbonyl index, (b) aromatic index, (c) sulfoxide index, and (d) comparison of functional group indices.

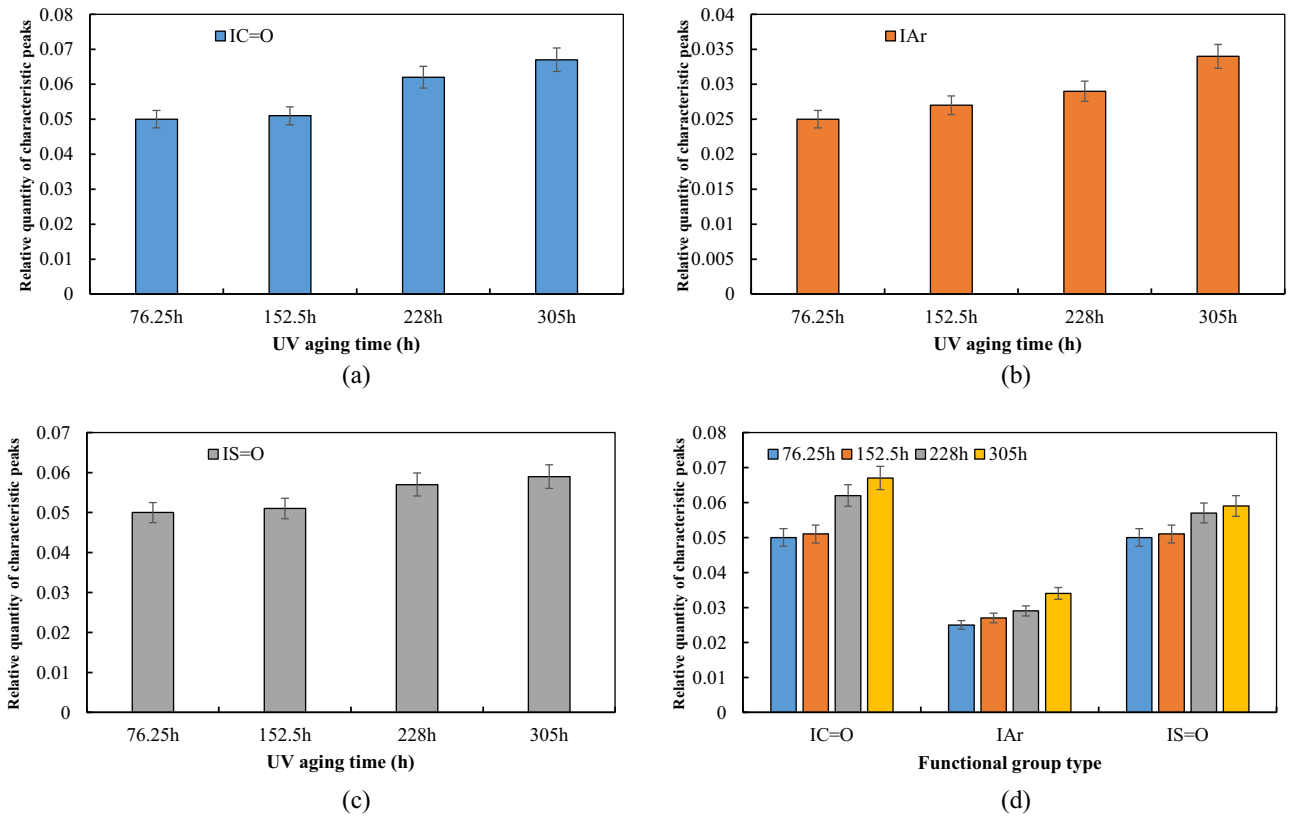

Figure 18: Characteristic functional group index of the modified asphalt under different aging times: (a) carbonyl index, (b) aromatic index, (c) sulfoxide index, and (d) comparison of functional group indices.

horizontal axis for the analysis. The larger the relative area of the calculated characteristic peak was, the deeper the impact of UV aging would be. The changes in the aging index of characteristic functional maps such as C═O sulfoxide group (1,030 cm^{-1}) and S═O carbonyl group (1,700 cm^{-1}) are defined and statistically analyzed. The calculation formula is shown in formula 2, and the results are shown in Figure 18.

$$\sum A = A_{1,700} + A_{1,645} + A_{1,601} + A_{1,458} + A_{1,378} + A_{1,144} + A_{1,030} + A_{962} + A_{895} + A_{808} + A_{744}. \quad (2)$$

As shown in Figure 18, during the UV aging process, there is usually an oxidation reaction accompanied by the production of sulfoxide and carbonyl groups. The growth trend of T770-modified asphalt aging index with different UV aging times was similar to that of 70# asphalt. The aging index of aromatic functional groups reached its lowest value among the four aging time points at 76.25 h, followed by a significant increase, reaching its maximum value at 305 h. The trend of changes in the carbonyl and sulfoxide indices is consistent, with a significant increase in their aging indices during the 305 h, indicating a positive correlation between aging time and aging indices. Although the modified asphalt mixed with hindered amine light stabilizer will still produce corresponding functional groups under the influence of ultraviolet radiation, the growth rate and exponential growth amount of the relevant functional group are significantly lower than those of the 70# asphalt. This shows that the hindered amine light stabilizer added can react with asphalt materials and make asphalt components produce aromatization changes. Meanwhile, it strengthens the overall stability of the internal colloidal structure of asphalt. Under the action of ultraviolet radiation, asphalt could show good antiaging performance.

3.5.2.3 Comparison analysis

Figure 19 presents a comparison of the characteristic functional group index between the 70# base asphalt and T770-modified asphalt. As shown in Figure 19, both the 70# base asphalt and T770-modified asphalt exhibit a significant increasing trend in their characteristic functional group index with the prolonged ultraviolet aging time. This indicates that ultraviolet radiation promotes the formation and accumulation of functional groups, such as carbonyl and sulfonyl groups, in the asphalt, leading to some degree of

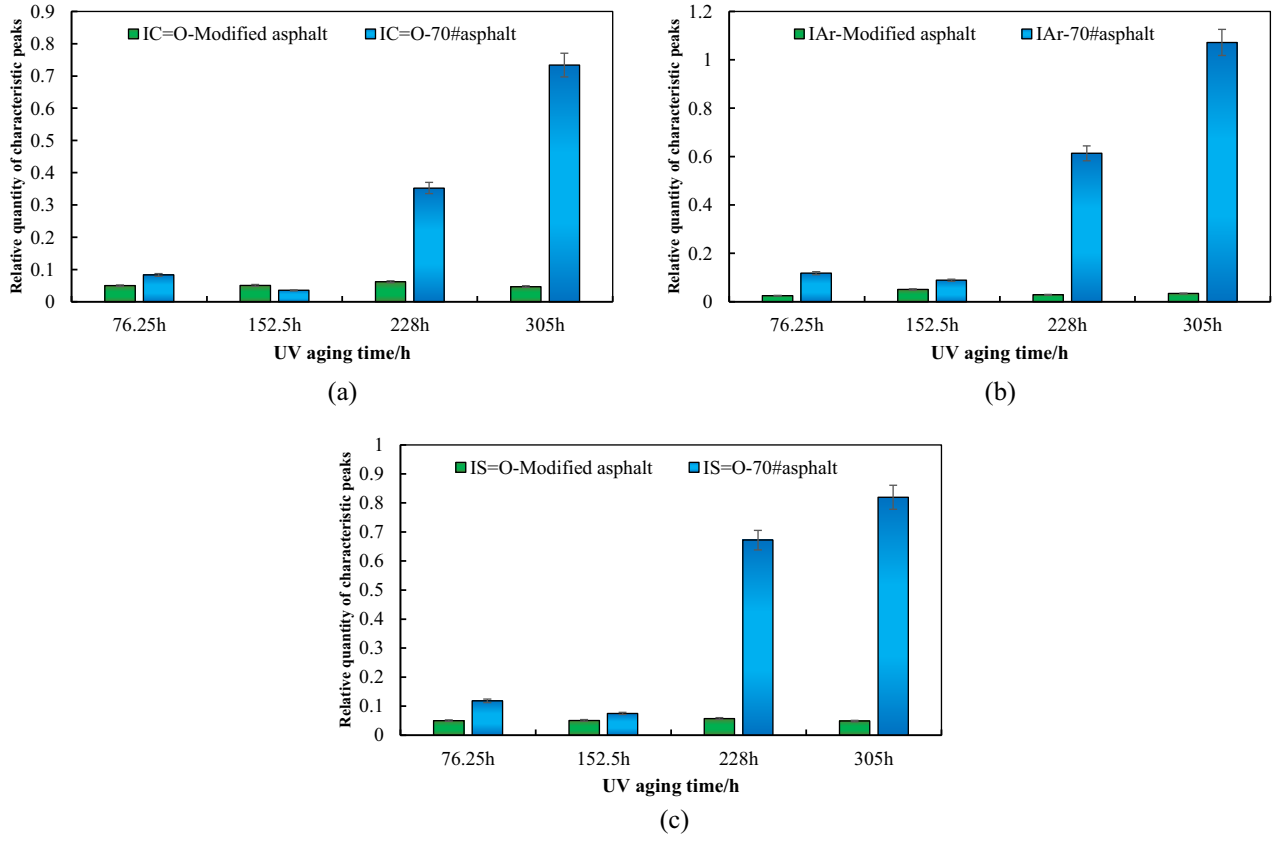

Figure 19: Characteristic functional group index comparison of UV-aged 70# asphalt and modified asphalt. (a) $I_{C=O}$, (b) I_{Ar}, and (c) $I_{S=O}$.

mutual transformation between different chemical components within the asphalt. Further analysis reveals that, during the early stages of ultraviolet aging (152.5 h), the difference in the characteristic functional group index between the 70# base asphalt and T770-modified asphalt is relatively small, with specific values around 43%. However, when the ultraviolet aging time exceeds 208 h, the difference between the two becomes highly significant, with the functional group index decreasing by more than 90%. This suggests that the addition of the T770 light stabilizer effectively inhibits the formation and accumulation of ultraviolet-induced characteristic functional groups within the asphalt, thereby suppressing the development of ultraviolet aging behavior and controlling the performance degradation caused by ultraviolet aging in the asphalt.

4 Conclusions

The main research conclusions of this article are as follows:

i) The ultraviolet aging effect could lead to the hardening of asphalt, manifested in the increase of softening point and the significant decrease in penetration and ductility at the performance level. Meanwhile, the increase of rutting factor also led to the enhancement of asphalt viscosity. The high content of T770 light stabilizer increases the UV radiation resistance of asphalt binder, which could mitigate the change amplitude of mechanical performances of asphalt material. The primary reason why the T770 light stabilizer enhances the antiaging performance of asphalt materials is its ability to neutralize free radicals generated during UV aging within the asphalt. This process reduces the accumulation of carbonyl, sulfoxide, and other functional groups, thereby inhibiting the transformation among the four components of asphalt. Subsequent FTIR test results further confirmed that the application of the T770 light stabilizer significantly reduced the index of characteristic functional groups.
ii) After the same UV aging time, the crack width of the matrix asphalt is larger. The degree of crack penetration and expansion is more severe compared to the light stabilized modified asphalt, and the UV aging phenomenon is more obvious. For T770-modified asphalt, the evolution process of its "crack structure" is slower, which means that T770 light stabilizer could delay the rate of change in asphalt surface morphology at the microlevel. The mitigation of microcracks on the asphalt surface may be attributed to the T770 modifier reducing the hardness of the asphalt material after UV aging, thereby improving the deformability of the asphalt binder. This optimization helps alleviate the formation and propagation of microcracks on the asphalt surface during UV aging.
iii) Compared to base asphalt, the addition of the T770 light stabilizer significantly reduced the indices of characteristic functional groups such as carbonyl and sulfoxide by more than 90%. This substantial reduction in the formation and accumulation of aging intermediates at the chemical composition level was also validated and reflected in the mechanical and rheological properties of asphalt. Hindered amine light stabilizer could react with asphalt materials and make asphalt components produce aromatization changes, while strengthening the overall stability of the internal colloidal structure of asphalt. Under the effect of ultraviolet radiation, good antiaging performance of asphalt could be improved, which could inhibit the aging behavior of 70# asphalt and the deterioration of road performance.
iv) Regarding the results of this study, future study would focus on the actual applying effect of HALS on asphalt pavement materials in engineering projects. Furthermore, the impact of high temperature mixing on HALS would be studied during the mixing process of asphalt mixture.

Acknowledgments: This article describes research activities mainly requested and sponsored by Opening Funding Supported by the Key Laboratory of Transport Industry of Road Structure and Material (Research Institute of Highway, Ministry of Transport, Beijing, PRC), Guangdong Basic and Applied Basic Research Foundation (2024A1515012242), Guangzhou Basic and Applied Basic Research Project (Young Doctor "Sailing" Project) (2024A04J1276). That sponsorship and interest are gratefully acknowledged.

Funding information: This article describes research activities mainly requested and sponsored by Opening Funding Supported by the Key Laboratory of Transport Industry of Road Structure and Material (Research Institute of Highway, Ministry of Transport, Beijing, PRC), Guangdong Basic and Applied Basic Research Foundation (2024A1515012242), Guangzhou Basic and Applied Basic Research Project (Young Doctor "Sailing" Project) (2024A04J1276).

Author contributions: All authors have accepted responsibility for the entire content of this manuscript and approved its submission.

Conflict of interest: The authors state no conflict of interest.

Data availability statement: The data that support the findings of this study are available from the corresponding author, upon reasonable request.

References

[1] Liang, M., M. Guo, Y. Tan, S. He, and X. Du. Evaluation of anti-aging performance of bitumen based on rheological and chemical characterization. *International Journal of Pavement Engineering*, Vol. 24, No. 1, 2023, id. 2213385.

[2] Zhang, H., H. Luo, H. Duan, and J. Cao. Influence of zinc oxide/expanded vermiculite composite on the rheological and anti-aging properties of bitumen. *Fuel*, Vol. 315, 2022, id. 123165.

[3] Yousefi, A., A. Behnood, A. Nowruzi, and H. Haghshenas. Performance evaluation of asphalt mixtures containing warm mix asphalt (WMA) additives and reclaimed asphalt pavement (RAP). *Construction and Building Materials*, Vol. 268, 2021, id. 121200.

[4] Sun, X., X. Qin, Z. Liu, and Y. Yin. Damaging effect of fine grinding treatment on the microstructure of polyurea elastomer modifier used in asphalt binder. *Measurement*, Vol. 2024, 2024, id. 115984.

[5] Li, Y., J. Feng, S. Wu, A. Chen, D. Kuang, T. Bai, et al. Review of ultraviolet aging mechanisms and anti-aging methods for asphalt binders. *Journal of Road Engineering*, Vol. 2, No. 2, 2022, pp. 137–155.

[6] Liu, Y., P. Su, M. Li, Z. You, and M. Zhao. Review on evolution and evaluation of asphalt pavement structures and materials. *Journal of Traffic and Transportation Engineering (English Edition)*, Vol. 7, No. 5, 2020, pp. 573–599.

[7] Polo-Mendoza, R., G. Martinez-Arguelles, L. F. Walubita, F. Moreno-Navarro, F. Giustozzi, L. Fuentes, et al. Ultraviolet aging of bituminous materials: A comprehensive literature review from 2011 to 2022. *Construction and Building Materials*, Vol. 350, 2022, id. 128889.

[8] El-Hiti, G. A., D. S. Ahmed, E. Yousif, O. S. Al-Khazrajy, M. Abdallh, and S. A. Alanazi. Modifications of polymers through the addition of ultraviolet absorbers to reduce the aging effect of accelerated and natural irradiation. *Polymers*, Vol. 14, No. 1, 2021, id. 20.

[9] Sun, X., J. Yuan, Z. Liu, X. Qin, and Y. Yin. Evaluation and characterization on the segregation and dispersion of anti-UV aging modifying agent in asphalt binder. *Construction and Building Materials*, Vol. 289, 2021, id. 123204.

[10] Duan, H., H. Kuang, H. Zhang, J. Liu, H. Luo, and J. Cao. Investigation on microstructure and aging resistance of bitumen modified by zinc oxide/expanded vermiculite composite synthesized with different methods. *Fuel*, Vol. 324, 2022, id. 124590.

[11] Luo, Y., H. Zhang, H. Duan, P. Du, and J. Cao. A novel method to improve anti-aging properties of SBS modified bitumen by zinc oxide/expanded vermiculite composite: Influence of zinc oxide particle loadings. *Construction and Building Materials*, Vol. 408, 2023, id. 133790.

[12] Ahmad, M., M. Khedmati, D. Mensching, B. Hofko, and H. F. Haghshenas. Aging characterization of asphalt binders through multi-aspect analyses: A critical review. *Fuel*, Vol. 376, 2024, id. 132679.

[13] Xu, S., G. Tang, S. Pan, Z. Ji, L. Fang, C. Zhang, et al. Application of reactive rejuvenator in aged SBS modified asphalt regeneration: A review. *Construction and Building Materials*, Vol. 421, 2024, id. 135696.

[14] Liu, Y. R., X. Tang, Q. Zeng, and J. P. Lai. Impacts of ultraviolet absorption by zinc oxide nanoparticle modifiers on asphalt aging. *Scientific Reports*, Vol. 14, No. 1, 2024, id. 19918.

[15] Ju, Z., D. Ge, Y. Xue, D. Duan, S. Lv, and S. Cao. Investigation of the influence of the variable-intensity ultraviolet aging on asphalt properties. *Construction and Building Materials*, Vol. 411, 2024, id. 134720.

[16] Zhao, W., G. Fang, X. Qin, and J. Mao. Multiscale characterization of the UV aging resistance and mechanism of light stabilizer-modified asphalt. *Reviews on Advanced Materials Science*, Vol. 63, No. 1, 2024, id. 20230152.

[17] Zheng, Q., P. He, D. Zhang, Y. Weng, J. Lu, and T. Wang. A holistic view of asphalt binder aging under ultraviolet conditions: Chemical, structural, and rheological characterization. *Buildings*, Vol. 14, No. 10, 2024, id. 3276.

[18] Pandhawale, S. S., S. Jain, A. K. Chandrappa, and V. Kari. UV aging assessment of asphalt binder: influence of duration, zinc oxide, and aging condition. *International Journal of Pavement Engineering*, Vol. 25, No. 1, 2024, id. 2359537.

[19] Enfrin, M. and F. Giustozzi. The role of polymer modification in mitigating 'sunburn'damage on asphalt roads. *Journal of Cleaner Production*, Vol. 439, 2024, id. 140929.

[20] Liu, Z., X. Sun, H. Xu, Y. Lu, Z. Su, Y. Ye, et al. Anti-aging performance and action mechanism of asphalt modified by composite modification. *Applied Sciences*, Vol. 14, No. 22, 2024, id. 10250.

[21] Sun, X., H. Xu, X. Qin, Y. Zhu, and J. Jin. Cross-scale study on the interaction behaviour of municipal solid waste incineration fly ash-asphalt mortar: A macro-micro approach. *International Journal of Pavement Engineering*, Vol. 26, No. 1, 2025, id. 2469114.

[22] Guo, M., M. Liang, and X. Du. Evaluation on feasibility of carbon black and hindered amine light stabilizer as UV-resistant additives of asphalt binder. *Journal of Testing and Evaluation*, Vol. 51, No. 6, 2023, 3987–4003.

[23] Gijsman, P. A review on the mechanism of action and applicability of Hindered Amine Stabilizers. *Polymer Degradation and Stability*, Vol. 145, 2017, pp. 2–10.

[24] Qian, G., G. Yuan, D. Zhang, and Z. Li. Effect of composite light stabilizer on the anti-ultraviolet aging property of matrix asphalt. *Journal of Materials in Civil Engineering*, Vol. 33, No. 8, 2021, id. 04021176.

[25] Li, X., J. Zhang, and S. Wang. Study on the anti-aging performance of asphalt modified with HALS. *Journal of Materials in Civil Engineering*, Vol. 31, No. 5, 2019, id. 04019031.

[26] Wang, Y., H. Liu, and F. Zhang. Effect of HALS on asphalt aging under high temperature and UV conditions. *Construction and Building Materials*, Vol. 250, 2020, id. 118776.

[27] Chen, Q., T. Ge, X. Li, X. Li, and C. Wang. Road area pollution cleaning technology for asphalt pavement: Literature review and research propositions. *Journal of Cleaner Production*, Vol. 493, 2025, id. 144975.

[28] Chen, L., X. Huang, and J. Wang. Synergistic effect of HALS and UV absorbers in asphalt aging. *Polymer Testing*, Vol. 93, 2021, id. 107005.

[29] Chen, Z., Z. Zhang, X. Chen, R. Hou, Z. Ding, F. Liu, et al. Multi-role collaborative framework for structural damage identification considering measurement noise effect. *Measurement*, Vol. 250, 2025, id. 117106.

[30] Wang, S., X. Ji, S. Li, Y. Tian, Y. Chen, and L. Liu. Synthesis and characterization of heat-force dual-induction nano-SiC modified microcapsule. *Construction and Building Materials*, Vol. 470, 2025, id. 140594.

[31] Zhang, S. and X. Liu. Microstructure and aging behavior of HALS in modified asphalt. *Journal of Applied Polymer Science*, Vol. 139, No. 12, 2022, id. 51960.

[32] Xu, H., W. Li, and D. Zhao. Field performance of HALS-modified asphalt in hot and UV-intensive climates. *Transportation Research Record*, Vol. 2677, No. 2, 2023, pp. 1–12.